Doping and temperature dependence of electron spectrum and quasiparticle dispersion in doped bilayer cuprates

Yu Lan
Department of Physics, Beijing Normal University, Beijing 100875, China

Jihong Qin
Department of Physics, Beijing University of Science and Technology, Beijing 100083, China

Shiping Feng
Department of Physics, Beijing Normal University, Beijing 100875, China

(Received 16 October 2006; revised manuscript received 24 January 2007; published 18 April 2007)

Within the t-t'-J model, the electron spectrum and quasiparticle dispersion in doped bilayer cuprates in the normal state are discussed by considering the bilayer interaction. It is shown that the bilayer interaction splits the electron spectrum of doped bilayer cuprates into the bonding and antibonding components around the $[\pi,0]$ point. The differentiation between the bonding and antibonding components is essential, which leads to two main flatbands around the $[\pi,0]$ point below the Fermi energy. In analogy to the doped single layer cuprates, the lowest energy states in doped bilayer cuprates are located at the $[\pi/2,\pi/2]$ point. Our results also show that the striking behavior of the electronic structure in doped bilayer cuprates is intriguingly related to the bilayer interaction together with strong coupling between the electron quasiparticles and collective magnetic excitations.

DOI: 10.1103/PhysRevB.75.134513 PACS number(s): 74.70.−b, 74.25.Jb, 74.20.Mn, 74.62.Dh

I. INTRODUCTION

Cuprate materials are unusual in that the undoped cuprates are insulators with an antiferromagnetic (AF) long-range order (AFLRO), and changing the carrier concentration by ionic substitution or increase of the oxygen content turns these compounds into correlated metals, leaving short-range AF correlations still intact.[1–5] The single common feature of cuprate superconductors is the presence of the two-dimensional CuO_2 plane,[1–5] and it seems evident that the unusual behaviors of doped cuprates are dominated by the CuO_2 plane.[6] This layered crystal structure stems from the fact that cuprate superconductors are highly anisotropic materials, so the electron spectral function $A(\mathbf{k},\omega)$ is dependent on the in-plane momentum.[1–5] After 20 years of extensive studies, it has been shown that many of the unusual physical properties have often been attributed to particular characteristics of low-energy excitations determined by the electronic structure.[3–5]

Although the electronic structure of doped cuprates is well established by now,[3–5] its full understanding is still a challenging issue. Experimentally, angle-resolved photoemission spectroscopy (ARPES) experiments have provided rather detailed information on the electronic structure of the doped single layer and bilayer cuprates.[3–5,7–12] An important issue is whether the behavior of the low-energy excitations determined by the electronic structure is universal or not. The early ARPES measurements[5,7,8] showed that the charge carriers doped into the parent compounds first enter into the $\mathbf{k}=[\pi/2,\pi/2]$ (in units of inverse lattice constant) point in the Brillouin zone. Moreover, the electron spectral function $A(\mathbf{k},\omega)$ has a flatband form as a function of energy ω for momentum $\mathbf{k}$ in the vicinity of the $[\pi,0]$ point, which leads to the unusual quasiparticle dispersion around the $[\pi,0]$ point with anomalously small changes of electron energy as a function of momentum.[5,7,8] Furthermore, this flatband is just below the Fermi energy. Recently, the improvements in the resolution of the ARPES experiments[3,4,9–11] allowed one to resolve additional features in the electron spectral function $A(\mathbf{k},\omega)$. Among these achievements is the observation of the bilayer splitting (BS) in doped bilayer cuprates in a wide doping range.[3,9–11] In this case, whether or not the electronic structure of doped cuprates can be influenced by the interaction between CuO_2 planes has been an interesting issue. The study of the electronic structure is complicated by the BS, that is, the BS of the CuO_2 plane derived the electronic structure in the bonding and antibonding bands due to the presence of CuO_2 bilayer blocks in the unit cell of doped bilayer cuprates.[9–11] The magnitude of the BS is doping independent and increases upon approaching the $[\pi,0]$ point, where the BS exhibits the largest value. As a result of the maximal BS at the $[\pi,0]$ point, there are two main flatbands around the $[\pi,0]$ point.[9–11] Moreover, it has been shown that a well pronounced peak-dip-hump structure in the electron spectrum of doped bilayer cuprates in the superconducting state is partially caused by the BS.[13,14] Theoretically, the electron-removal spectral functions at the $[\pi,0]$ point and the quasiparticle dispersion of the multilayer cuprates in the normal state have been discussed[15] within the two-dimensional multilayer t-t'-t''-J model based on the resonating valence bond wave function and Gutzwiller approximation, in particular, their results show that there are two main flatbands around the $[\pi,0]$ point in the bilayer system. However, the resonating valence bond wave function and Gutzwiller approximation can only be applied to discuss the zero-temperature physical properties of doped cuprates. To the best of our knowledge, the doping and temperature dependence of the electron spectrum and quasiparticle dispersion

in both doped single layer and bilayer cuprates have not been treated from a unified point of view for the normal state.

In our earlier work using the charge-spin separation (CSS) fermion-spin theory,[16] the electronic structure of the doped single layer cuprates has been calculated within the single layer t-t'-J model,[17] and the obtained doping dependence of the electron spectrum and quasiparticle dispersion are consistent with the corresponding ARPES experiments.[5,7,8] In this paper, we show explicitly that if the bilayer interaction is included, one can reproduce some main features in the normal state such as observed experimentally on doped bilayer cuprates.[3,9–11] The differentiation between the bonding and antibonding components is essential. Two main flatbands around the $[\pi,0]$ point are rather similar to the scenario argued in Refs. 9, 10, and 15 for the normal state, and the quasiparticle dispersion we derive from the bilayer t-t'-J model (without additional terms and adjustable parameters) demonstrates explicitly this energy-band splitting. In comparison with the case of the doped single layer cuprates,[17] our present results also show that the striking behavior of the electronic structure in doped bilayer cuprates is intriguingly related to the bilayer interaction, together with strong coupling between the electron quasiparticles and collective magnetic excitations.

The rest of this paper is organized as follows. In Sec. II, we introduce the bilayer t-t'-J model that includes the bilayer hopping and bilayer magnetic exchange interaction. Within this bilayer t-t'-J model, we calculate explicitly the longitudinal and transverse components of the electron Green's functions based on the CSS fermion-spin theory by considering charge-carrier fluctuations, and then obtain the bonding and antibonding electron spectral functions according to these longitudinal and transverse components of the electron Green's functions. The doping and temperature dependence of the electron spectrum and quasiparticle dispersion of doped bilayer cuprates in the normal state are presented in Sec. III. Section IV is devoted to a summary and discussions.

II. THEORETICAL FRAMEWORK

The basic element of cuprate materials is a two-dimensional CuO_2 plane, and it is believed that the unusual behaviors of doped cuprates are closely related to the doped CuO_2 plane as mentioned above.[1–5] It has been argued that the essential physics of the doped CuO_2 plane is contained in the t-t'-J model on a square lattice.[6] In this case, the t-t'-J model in the bilayer structure is expressed as

$$H = -t\sum_{i\hat{\eta}a\sigma} C^{\dagger}_{ia\sigma}C_{i+\hat{\eta}a\sigma} + t'\sum_{i\hat{\tau}a\sigma} C^{\dagger}_{ia\sigma}C_{i+\hat{\tau}a\sigma} - \sum_{i\sigma} t_{\perp}(i)(C^{\dagger}_{i1\sigma}C_{i2\sigma} + \text{H.c.}) + \mu\sum_{ia\sigma} C^{\dagger}_{ia\sigma}C_{ia\sigma} + J\sum_{i\hat{\eta}a} \mathbf{S}_{ia}\cdot\mathbf{S}_{i+\hat{\eta}a} + J_{\perp}\sum_{i} \mathbf{S}_{i1}\cdot\mathbf{S}_{i2}, \tag{1}$$

where $\hat{\eta}=\pm\hat{x},\pm\hat{y}$, $\hat{\tau}=\pm\hat{x}\pm\hat{y}$, $a=1,2$ is the plane index, $C^{\dagger}_{ia\sigma}$ ($C_{ia\sigma}$) is the electron creation (annihilation) operator, $\mathbf{S}_{ia}=C^{\dagger}_{ia}\vec{\sigma}C_{ia}/2$ is the spin operator with $\vec{\sigma}=(\sigma_x,\sigma_y,\sigma_z)$ as Pauli matrices, μ is the chemical potential, and the interlayer hopping,[18]

$$t_{\perp}(\mathbf{k}) = \frac{t_{\perp}}{4}(\cos k_x - \cos k_y)^2, \tag{2}$$

describes coherent hopping between the CuO_2 planes. This functional form of the interlayer hopping in Eq. (2) is predicted on the basis of the local-density approximation calculations,[18] and, as will be shown later, the experimentally observed BS agrees well with it.[3,9–11] The t-t'-J Hamiltonian (1) is supplemented by the single occupancy local constraint $\sum_{\sigma}C^{\dagger}_{ia\sigma}C_{ia\sigma}\leq 1$. This local constraint can be treated properly in analytical calculations within the CSS fermion-spin theory,[16] where the constrained electron operators in the t-J type model are decoupled as $C_{ia\uparrow}=h^{\dagger}_{ia\uparrow}S^{-}_{ia}$ and $C_{ia\downarrow}=h^{\dagger}_{ia\downarrow}S^{+}_{ia}$, with the spinful fermion operator $h_{ia\sigma}=e^{-i\Phi_{ia\sigma}}h_{ia}$ keeping track of the charge degree of freedom together with some effects of the spin-configuration rearrangements due to the presence of the doped hole itself (dressed holon), while the spin operator S_{ia} keeps track of the spin degree of freedom. The advantage of this CSS fermion-spin theory is that the electron local constraint for single occupancy, $\sum_{\sigma}C^{\dagger}_{ia\sigma}C_{ia\sigma}=S^{+}_{ia}h_{ia\uparrow}h^{\dagger}_{ia\uparrow}S^{-}_{ia}+S^{-}_{ia}h_{ia\downarrow}h^{\dagger}_{ia\downarrow}S^{+}_{ia}=h_{ia}h^{\dagger}_{ia}(S^{+}_{ia}S^{-}_{ia}+S^{-}_{ia}S^{+}_{ia})=1-h^{\dagger}_{ia}h_{ia}\leq 1$, is satisfied in analytical calculations, and the double spinful fermion occupancies $h^{\dagger}_{ia\sigma}h^{\dagger}_{ia-\sigma}=e^{i\Phi_{ia\sigma}}h^{\dagger}_{ia}h^{\dagger}_{ia}e^{i\Phi_{ia-\sigma}}=0$ and $h_{ia\sigma}h_{ia-\sigma}=e^{-i\Phi_{ia\sigma}}h_{ia}h_{ia}e^{-i\Phi_{ia-\sigma}}=0$, are ruled out automatically. It has been shown[16] that these dressed holons and spins are gauge invariant, and in this sense, they are real and can be interpreted as the physical excitations.[19] Although in common sense $h_{ia\sigma}$ is not a real spinful fermion, it behaves like a spinful fermion. In this CSS fermion-spin representation, the low-energy behavior of the bilayer t-t'-J Hamiltonian (1) can be expressed as

$$\begin{aligned} H = {} & t\sum_{i\hat{\eta}a}(h^{\dagger}_{i+\hat{\eta}a\uparrow}h_{ia\uparrow}S^{+}_{ia}S^{-}_{i+\hat{\eta}a} + h^{\dagger}_{i+\hat{\eta}a\downarrow}h_{ia\downarrow}S^{-}_{ia}S^{+}_{i+\hat{\eta}a}) \\ & - t'\sum_{i\hat{\tau}a}(h^{\dagger}_{i+\hat{\tau}a\uparrow}h_{ia\uparrow}S^{+}_{ia}S^{-}_{i+\hat{\tau}a} + h^{\dagger}_{i+\hat{\tau}a\downarrow}h_{ia\downarrow}S^{-}_{ia}S^{+}_{i+\hat{\tau}a}) \\ & + \sum_{i} t_{\perp}(i)(h^{\dagger}_{i2\uparrow}h_{i1\uparrow}S^{+}_{i1}S^{-}_{i2} + h^{\dagger}_{i1\uparrow}h_{i2\uparrow}S^{+}_{i2}S^{-}_{i1} \\ & + h^{\dagger}_{i2\downarrow}h_{i1\downarrow}S^{-}_{i1}S^{+}_{i2} + h^{\dagger}_{i1\downarrow}h_{i2\downarrow}S^{-}_{i2}S^{+}_{i1}) \\ & - \mu\sum_{ia\sigma} h^{\dagger}_{ia\sigma}h_{ia\sigma} + J_{\text{eff}}\sum_{i\hat{\eta}a}\mathbf{S}_{ia}\cdot\mathbf{S}_{i+\hat{\eta}a} + J_{\text{eff}\perp}\sum_{i}\mathbf{S}_{i1}\cdot\mathbf{S}_{i2}, \end{aligned} \tag{3}$$

where $J_{\text{eff}}=J(1-\delta)^2$, $J_{\text{eff}\perp}=J_{\perp}(1-\delta)^2$, and $\delta=\langle h^{\dagger}_{ia\sigma}h_{ia\sigma}\rangle=\langle h^{\dagger}_{ia}h_{ia}\rangle$ is the hole doping concentration. As a result, the magnetic energy term in the bilayer t-t'-J model is only considered to form an adequate spin configuration,[20] while the kinetic energy part has been expressed as the interaction between the dressed holons and spins; this interaction dominates the essential physics of doped cuprates.[16]

Within the CSS fermion-spin theory, the electron spectral function and related quasiparticle dispersion of the doped single layer cuprates in the normal state have been discussed by considering the dressed holon fluctuations around the mean-field (MF) solution,[17] where the spin part is limited to first order (the MF level), while the full dressed holon

Green's function is treated self-consistently in terms of Eliashberg's strong-coupling theory.[21] For doped bilayer cuprates, there are two coupled CuO_2 planes in the unit cell. This stems from the fact that the energy spectrum has two branches, so the dressed holon and spin Green's functions are matrices and can be expressed as $g(\mathbf{k},\omega)=g_L(\mathbf{k},\omega)+\sigma_x g_T(\mathbf{k},\omega)$ and $D(\mathbf{k},\omega)=D_L(\mathbf{k},\omega)+\sigma_x D_T(\mathbf{k},\omega)$, respectively, where the longitudinal and transverse parts correspond to the in-layer and interlayer Green's functions.[22] In this case, we follow the previous discussions for the single layer case[17] and obtain explicitly the longitudinal and transverse parts of the full dressed holon Green's functions of the doped bilayer system as (see the Appendix)

$$g_L(\mathbf{k},\omega)=\frac{1}{2}\sum_{\nu=1,2}\frac{Z_{FA}^{(\nu)}}{\omega-\bar{\xi}_{\nu\mathbf{k}}}, \tag{4a}$$

$$g_T(\mathbf{k},\omega)=\frac{1}{2}\sum_{\nu=1,2}(-1)^{\nu+1}\frac{Z_{FA}^{(\nu)}}{\omega-\bar{\xi}_{\nu\mathbf{k}}}, \tag{4b}$$

with the renormalized dressed holon excitation spectrum $\bar{\xi}_{\nu\mathbf{k}}=Z_{FA}^{(\nu)}\xi_{\nu\mathbf{k}}$, where the MF dressed holon excitation spectrum is given as

$$\xi_{\nu\mathbf{k}}=Zt\chi_1\gamma_{\mathbf{k}}-Zt'\chi_2\gamma'_{\mathbf{k}}-\mu+(-1)^{\nu+1}\chi_\perp t_\perp(\mathbf{k}); \tag{5}$$

with the spin-correlation functions $\chi_1=\langle S_{ia}^+S_{i+\hat{\eta}a}^-\rangle$, $\chi_2=\langle S_{ia}^+S_{i+\hat{\tau}a}^-\rangle$, and $\chi_\perp=\langle S_{i1}^+S_{i2}^-\rangle$; $\gamma_{\mathbf{k}}=(1/Z)\Sigma_{\hat{\eta}}e^{i\mathbf{k}\cdot\hat{\eta}}$, $\gamma'_{\mathbf{k}}=(1/Z)\Sigma_{\hat{\tau}}e^{i\mathbf{k}\cdot\hat{\tau}}$, and Z is the number of the nearest-neighbor or second-nearest-neighbor sites. The quasiparticle coherent weights $Z_{FA}^{(1)-1}=Z_{F1}^{-1}-Z_{F2}^{-1}$ and $Z_{FA}^{(2)-1}=Z_{F1}^{-1}+Z_{F2}^{-1}$, with $Z_{F1}^{-1}=1-\Sigma_L^{(ho)}(\mathbf{k}_0,\omega)|_{\omega=0}$, $Z_{F2}^{-1}=\Sigma_T^{(ho)}(\mathbf{k}_0,\omega)|_{\omega=0}$, and $\mathbf{k}_0=[\pi/2,\pi/2]$, where $\Sigma_L^{(ho)}(\mathbf{k},\omega)$ and $\Sigma_T^{(ho)}(\mathbf{k},\omega)$ are the corresponding antisymmetric parts of the longitudinal and transverse dressed holon self-energy functions,

$$\Sigma_L^{(h)}(\mathbf{k},i\omega_n)=\frac{1}{N^2}\sum_{\mathbf{p},\mathbf{q}}\Bigg[R_{\mathbf{p}+\mathbf{q}+\mathbf{k}}^{(1)}\frac{1}{\beta}\sum_{ip_m}g_L(\mathbf{p}+\mathbf{k},ip_m+i\omega_n)\times\Pi_{LL}(\mathbf{p},\mathbf{q},ip_m)+R_{\mathbf{p}+\mathbf{q}+\mathbf{k}}^{(2)}\times\frac{1}{\beta}\sum_{ip_m}g_T(\mathbf{p}+\mathbf{k},ip_m+i\omega_n)\times\Pi_{TL}(\mathbf{p},\mathbf{q},ip_m)\Bigg], \tag{6a}$$

$$\Sigma_T^{(h)}(\mathbf{k},i\omega_n)=\frac{1}{N^2}\sum_{\mathbf{p},\mathbf{q}}\Bigg[R_{\mathbf{p}+\mathbf{q}+\mathbf{k}}^{(1)}\frac{1}{\beta}\sum_{ip_m}g_T(\mathbf{p}+\mathbf{k},ip_m+i\omega_n)\times\Pi_{TT}(\mathbf{p},\mathbf{q},ip_m)+R_{\mathbf{p}+\mathbf{q}+\mathbf{k}}^{(2)}\times\frac{1}{\beta}\sum_{ip_m}g_L(\mathbf{p}+\mathbf{k},ip_m+i\omega_n)\times\Pi_{LT}(\mathbf{p},\mathbf{q},ip_m)\Bigg], \tag{6b}$$

with $R_{\mathbf{k}}^{(1)}=[Z(t\gamma_{\mathbf{k}}-t'\gamma'_{\mathbf{k}})]^2+t_\perp^2(\mathbf{k})$, $R_{\mathbf{k}}^{(2)}=2Z(t\gamma_{\mathbf{k}}-t'\gamma'_{\mathbf{k}})t_\perp(\mathbf{k})$, and the spin bubbles $\Pi_{\eta,\eta'}(\mathbf{p},\mathbf{q},ip_m)=(1/\beta)\Sigma_{iq_m}D_\eta^{(0)}\times(\mathbf{q},iq_m)D_{\eta'}^{(0)}(\mathbf{q}+\mathbf{p},iq_m+ip_m)$, where $\eta=L,T$ and $\eta'=L,T$. The longitudinal and transverse parts of the MF spin Green's functions are

$$D_L^{(0)}(\mathbf{k},\omega)=\frac{1}{2}\sum_{\nu=1,2}\frac{B_{\nu\mathbf{k}}}{\omega^2-\omega_{\nu\mathbf{k}}^2}, \tag{7a}$$

$$D_T^{(0)}(\mathbf{k},\omega)=\frac{1}{2}\sum_{\nu=1,2}(-1)^{\nu+1}\frac{B_{\nu\mathbf{k}}}{\omega^2-\omega_{\nu\mathbf{k}}^2}, \tag{7b}$$

with $B_{\nu\mathbf{k}}=\lambda(2\epsilon_\parallel\chi_1^z+\chi_1)\gamma_{\mathbf{k}}-2\lambda'\chi_2^z\gamma'_{\mathbf{k}}-J_{\mathrm{eff}\perp}[\chi_\perp+2\chi_\perp^z(-1)^\nu]\epsilon_\perp(\mathbf{k})-\lambda(\epsilon_\parallel\chi_1+2\chi_1^z)+\lambda'\chi_2-J_{\mathrm{eff}\perp}[2\chi_\perp^z+\chi_\perp(-1)^\nu]$, $\lambda=2ZJ_{\mathrm{eff}}$, $\lambda'=4Z\phi_2t'$, $\epsilon_\parallel=1+2t\phi_1/J_{\mathrm{eff}}$, $\epsilon_\perp(\mathbf{k})=1+4\phi_\perp t_\perp(\mathbf{k})/J_{\mathrm{eff}\perp}$; the spin-correlation functions $\chi_1^z=\langle S_{ia}^zS_{i+\hat{\eta}a}^z\rangle$, $\chi_2^z=\langle S_{ia}^zS_{i+\hat{\tau}a}^z\rangle$, and $\chi_\perp^z=\langle S_{i1}^zS_{i2}^z\rangle$; the dressed holon particle-hole order parameters $\phi_1=\langle h_{ia\sigma}^\dagger h_{i+\hat{\eta}a\sigma}\rangle$, $\phi_2=\langle h_{ia\sigma}^\dagger h_{i+\hat{\tau}a\sigma}\rangle$, and $\phi_\perp=\langle h_{i1\sigma}^\dagger h_{i2\sigma}\rangle$; and the MF dressed spin excitation spectrum,

$$\begin{aligned}\omega_{\nu\mathbf{k}}^2=&\lambda^2\Bigg[\Big(A_2-\alpha\epsilon_\parallel\chi_1^z\gamma_{\mathbf{k}}-\frac{1}{2Z}\alpha\epsilon_\parallel\chi_1\Big)(1-\epsilon_\parallel\gamma_{\mathbf{k}})+\frac{1}{2}\epsilon_\parallel\Big(A_1-\frac{2}{Z}\alpha\chi_1^z-\alpha\chi_1\gamma_{\mathbf{k}}\Big)(\epsilon_\parallel-\gamma_{\mathbf{k}})\Bigg]+\lambda'^2\Bigg[\alpha\Big(\chi_2^z\gamma'_{\mathbf{k}}-\frac{Z-1}{2Z}\chi_2\Big)\gamma'_{\mathbf{k}}\\&+\frac{1}{2}\Big(A_3-\frac{2}{Z}\alpha\chi_2^z\Big)\Bigg]+\lambda\lambda'\alpha\Bigg[\chi_1^z(1-\epsilon_\parallel\gamma_{\mathbf{k}})\gamma'_{\mathbf{k}}+\frac{1}{2}(\chi_1\gamma'_{\mathbf{k}}-C_2)(\epsilon_\parallel-\gamma_{\mathbf{k}})+\gamma'_{\mathbf{k}}(C_2^z-\epsilon_\parallel\chi_2^z\gamma_{\mathbf{k}})-\frac{1}{2}\epsilon_\parallel(C_2-\chi_2\gamma_{\mathbf{k}})\Bigg]\\&+\lambda J_{\mathrm{eff}\perp}\alpha\Bigg\{\frac{1}{2}C_\perp\epsilon_\perp(\mathbf{k})(\epsilon_\parallel-\gamma_{\mathbf{k}})+\frac{1}{2}\epsilon_\parallel\epsilon_\perp(\mathbf{k})(C_\perp-\chi_\perp\gamma_{\mathbf{k}})+C_\perp^z(1-\epsilon_\parallel\gamma_{\mathbf{k}})+(C_\perp^z-\epsilon_\parallel\chi_\perp^z\gamma_{\mathbf{k}})+(-1)^\nu\Bigg[\frac{1}{2}\chi_1\epsilon_\perp(\mathbf{k})(\epsilon_\parallel-\gamma_{\mathbf{k}})\\&+\frac{1}{2}\epsilon_\parallel(C_\perp-\chi_\perp\gamma_{\mathbf{k}})+\chi_1^z\epsilon_\perp(\mathbf{k})(1-\epsilon_\parallel\gamma_{\mathbf{k}})+\epsilon_\perp(\mathbf{k})(C_\perp^z-\epsilon_\parallel\chi_\perp^z\gamma_{\mathbf{k}})\Bigg]\Bigg\}+\lambda' J_{\mathrm{eff}\perp}\alpha\Bigg\{\epsilon_\perp(\mathbf{k})\Big(\frac{1}{2}\chi_\perp\gamma'_{\mathbf{k}}-C'_\perp\Big)+(C'^z_\perp+\chi_\perp^z)\gamma'_{\mathbf{k}}\\&+(-1)^\nu\Bigg[\epsilon_\perp(\mathbf{k})(\chi_2^z+\chi_\perp^z)\gamma'_{\mathbf{k}}-\frac{1}{2}[\chi_2\epsilon_\perp(\mathbf{k})-\chi_\perp\gamma'_{\mathbf{k}}]-\frac{1}{2}C'_\perp\Bigg]\Bigg\}+\frac{1}{4}J_{\mathrm{eff}\perp}^2[\epsilon_\perp(\mathbf{k})+(-1)^\nu]^2,\end{aligned} \tag{8}$$

where $A_1=\alpha C_1+(1-\alpha)/2Z$, $A_2=\alpha C_1^z+(1-\alpha)/4Z$, $A_3=\alpha C_3+(1-\alpha)/2Z$, and the spin-correlation functions $C_1=(1/Z^2)\Sigma_{\hat{\eta}\hat{\eta}'}\langle S^+_{i+\hat{\eta}a}S^-_{i+\hat{\eta}'a}\rangle$, $C_2=(1/Z^2)\Sigma_{\hat{\eta}\hat{\tau}}\langle S^+_{i+\hat{\eta}a}S^-_{i+\hat{\tau}a}\rangle$, $C_3=(1/Z^2)\Sigma_{\hat{\tau}\hat{\tau}'}\langle S^+_{i+\hat{\tau}a}S^-_{i+\hat{\tau}'a}\rangle$, $C_1^z=(1/Z^2)\Sigma_{\hat{\eta}\hat{\eta}'}\langle S^z_{i+\hat{\eta}a}S^z_{i+\hat{\eta}'a}\rangle$, $C_2^z=(1/Z^2)\Sigma_{\hat{\eta}\hat{\tau}}\langle S^z_{i+\hat{\eta}a}S^z_{i+\hat{\tau}a}\rangle$, $C_\perp=(1/Z)\Sigma_{\hat{\eta}}\langle S^+_{i1}S^-_{i+\hat{\eta}2}\rangle$, $C'_\perp=(1/Z)\Sigma_{\hat{\tau}}\langle S^+_{i1}S^-_{i+\hat{\tau}2}\rangle$, $C_\perp^z=(1/Z)\Sigma_{\hat{\eta}}\langle S^z_{i1}S^z_{i+\hat{\eta}2}\rangle$, and $C'^z_\perp=(1/Z)\Sigma_{\hat{\tau}}\langle S^z_{i1}S^z_{i+\hat{\tau}2}\rangle$. In order not to violate the sum rule of the correlation function $\langle S_i^+S_i^-\rangle=1/2$ in the case without AFLRO, the important decoupling parameter α has been introduced in the above MF calculation, which can be regarded as the vertex correction.[23]

For discussions of the electronic structure of doped bilayer cuprates in the normal state, we need to calculate the electron Green's function $G(i-j,t-t')=\langle\langle C_{i\sigma}(t);C^\dagger_{j\sigma}(t')\rangle\rangle=G_L(i-j,t-t')+\sigma_xG_T(i-j,t-t')$, which is a convolution of the spin Green's function and dressed holon Green's function in the CSS fermion-spin theory, and reflect the charge-spin recombination.[20] In the present bilayer system, the longitudinal and transverse parts of the electron Green's function can be obtained explicitly in terms of the corresponding MF spin Green's functions (7) and full dressed holon Green's functions (4) as

$$G_L(\mathbf{k},\omega)=\frac{1}{8N}\sum_{\mathbf{p}}\sum_{\mu\nu}Z_{FA}^{(\mu)}\frac{B_{\nu\mathbf{p}}}{\omega_{\nu\mathbf{p}}}\times\left[\frac{L^{(1)}_{\mu\nu}(\mathbf{k},\mathbf{p})}{\omega+\bar{\xi}_{\mu\mathbf{p}-\mathbf{k}}-\omega_{\nu\mathbf{p}}}+\frac{L^{(2)}_{\mu\nu}(\mathbf{k},\mathbf{p})}{\omega+\bar{\xi}_{\mu\mathbf{p}-\mathbf{k}}+\omega_{\nu\mathbf{p}}}\right],\tag{9a}$$

$$G_T(\mathbf{k},\omega)=\frac{1}{8N}\sum_{\mathbf{p}}\sum_{\mu\nu}(-1)^{\mu+\nu}Z_{FA}^{(\mu)}\frac{B_{\nu\mathbf{p}}}{\omega_{\nu\mathbf{p}}}\times\left[\frac{L^{(1)}_{\mu\nu}(\mathbf{k},\mathbf{p})}{\omega+\bar{\xi}_{\mu\mathbf{p}-\mathbf{k}}-\omega_{\nu\mathbf{p}}}+\frac{L^{(2)}_{\mu\nu}(\mathbf{k},\mathbf{p})}{\omega+\bar{\xi}_{\mu\mathbf{p}-\mathbf{k}}+\omega_{\nu\mathbf{p}}}\right],\tag{9b}$$

where $L^{(1)}_{\mu\nu}(\mathbf{k},\mathbf{p})=n_F(\bar{\xi}_{\mu\mathbf{p}-\mathbf{k}})+n_B(\omega_{\nu\mathbf{p}})$, $L^{(2)}_{\mu\nu}(\mathbf{k},\mathbf{p})=1-n_F(\bar{\xi}_{\mu\mathbf{p}-\mathbf{k}})+n_B(\omega_{\nu\mathbf{p}})$, and $n_B(\omega)$ and $n_F(\omega)$ are the boson and fermion distribution functions, respectively. Then the longitudinal and transverse electron spectral functions $A_L(\mathbf{k},\omega)=-2\,\mathrm{Im}\,G_L(\mathbf{k},\omega)$ and $A_T(\mathbf{k},\omega)=-2\,\mathrm{Im}\,G_T(\mathbf{k},\omega)$ are obtained from the above longitudinal and transverse electron Green's functions as

$$A_L(\mathbf{k},\omega)=\pi\frac{1}{4N}\sum_{\mathbf{p}}\sum_{\mu\nu}Z_{FA}^{(\mu)}\frac{B_{\nu\mathbf{p}}}{\omega_{\nu\mathbf{p}}}[L^{(1)}_{\mu\nu}(\mathbf{k},\mathbf{p})\,\delta(\omega+\bar{\xi}_{\mu\mathbf{p}-\mathbf{k}}-\omega_{\nu\mathbf{p}})+L^{(2)}_{\mu\nu}(\mathbf{k},\mathbf{p})\,\delta(\omega+\bar{\xi}_{\mu\mathbf{p}-\mathbf{k}}+\omega_{\nu\mathbf{p}})],\tag{10a}$$

$$A_T(\mathbf{k},\omega)=\pi\frac{1}{4N}\sum_{\mathbf{p}}\sum_{\mu\nu}(-1)^{\mu+\nu}Z_{FA}^{(\mu)}\frac{B_{\nu\mathbf{p}}}{\omega_{\nu\mathbf{p}}}\times[L^{(1)}_{\mu\nu}(\mathbf{k},\mathbf{p})\,\delta(\omega+\bar{\xi}_{\mu\mathbf{p}-\mathbf{k}}-\omega_{\nu\mathbf{p}})+L^{(2)}_{\mu\nu}(\mathbf{k},\mathbf{p})\,\delta(\omega+\bar{\xi}_{\mu\mathbf{p}-\mathbf{k}}+\omega_{\nu\mathbf{p}})].\tag{10b}$$

With the help of the above longitudinal and transverse electron spectral functions, the bonding and antibonding electron spectral functions of doped bilayer cuprates are obtained as

$$A^+(\mathbf{k},\omega)=\frac{1}{2}[A_L(\mathbf{k},\omega)+A_T(\mathbf{k},\omega)],\tag{11a}$$

$$A^-(\mathbf{k},\omega)=\frac{1}{2}[A_L(\mathbf{k},\omega)-A_T(\mathbf{k},\omega)],\tag{11b}$$

respectively.

III. ELECTRON SPECTRUM AND QUASIPARTICLE DISPERSION OF DOPED BILAYER CUPRATES

We are now ready to discuss the doping and temperature dependence of the electron spectrum and quasiparticle dispersion of bilayer cuprate superconductors in the normal state. We have performed a calculation for the electron spectral functions in Eq. (11), and the results of the bonding (solid line) and antibonding (dashed line) electron spectral functions at (a) the $[\pi,0]$ point and (b) the $[\pi/2,\pi/2]$ point for parameters $t/J=2.5$, $t'/t=0.15$, and $t_\perp/t=0.3$ with temperature $T=0.1J$ at the doping concentration $\delta=0.15$ are plotted in Fig. 1. Apparently, there is a double-peak structure in the electron spectral function around the $[\pi,0]$ point, i.e., the bonding and antibonding quasiparticle peaks around the $[\pi,0]$ point are located at different positions, while the bonding and antibonding peaks around the $[\pi/2,\pi/2]$ point are located at the same position, which leads to the BS appearing around the $[\pi,0]$ point and it being absent in the vicinity of the $[\pi/2,\pi/2]$ point. In particular, the positions of the antibonding peaks at the $[\pi,0]$ point are more closer to the Fermi energy than those of the bonding peaks. In this sense, the differentiation between the bonding and antibonding components of the electron spectral function around the $[\pi,0]$ point is essential. In analogy to the single layer cuprates,[17] both positions of the quasiparticle peaks from the bonding and antibonding electron spectral functions at the $[\pi,0]$ and $[\pi/2,\pi/2]$ points are below the Fermi energy, but the positions of the peaks at the $[\pi/2,\pi/2]$ point are more closer to the Fermi energy, which indicates that the lowest energy states are located at the $[\pi/2,\pi/2]$ point. In other words, the low-energy spectral weight with the majority contribution to the low-energy properties of doped bilayer cuprates comes from the $[\pi/2,\pi/2]$ point. In qualitative agreement with the ARPES experimental data on doped bilayer cuprates.[3,9–11] The double-peak structure in the electron spectral functions around the $[\pi,0]$ point is closely related to the interlayer hopping form in Eq. (2). With decreasing values of $t_\perp$ and $J_\perp$, the distance between the bonding and antibonding peaks in the electron spectral functions decreases. When $t_\perp=0$ and $J_\perp=0$, we find that the transverse part of the dressed holon Green's functions in Eq. (4b) [hence the transverse part of the electron Green's functions in Eq. (9b) and the transverse part of the electron spectral functions in Eq. (10b)] is equal to zero. In this case, the bonding electron spectral function in Eq. (11a) is exactly the same as the antibonding

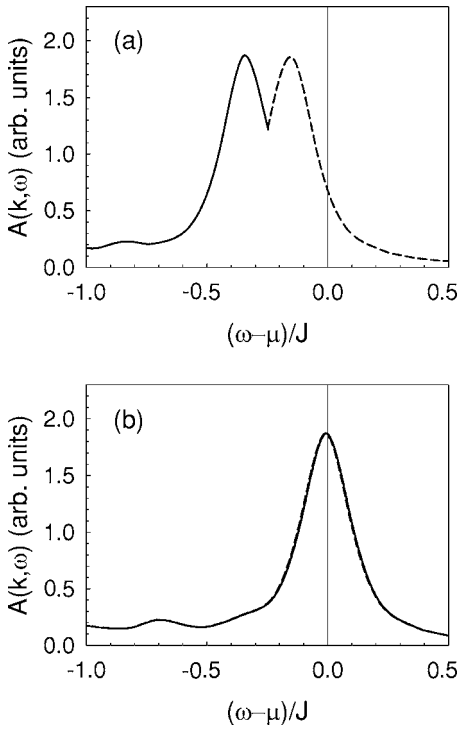

FIG. 1. The bonding (solid line) and antibonding (dashed line) electron spectral functions as a function of energy at (a) the $[\pi,0]$ point and (b) the $[\pi/2,\pi/2]$ point for $t/J=2.5$, $t'/t=0.15$, and $t_\perp/t=0.3$ with $T=0.1J$ at $\delta=0.15$.

electron spectral function in Eq. (11b), hence the electron spectral functions are reduced to the doped single layer case.[17]

For a better understanding of the physical properties of the electron spectrum in doped bilayer cuprates, we have studied the electron spectrum at different doping concentrations. The result of the electron spectral functions at $[\pi,0]$ point for $t/J=2.5$, $t'/t=0.15$, and $t_\perp/t=0.3$ with $T=0.1J$ at $\delta=0.09$ (solid line), $\delta=0.12$ (dashed line), and $\delta=0.15$ (dotted line) are plotted in Fig. 2, which indicates that with increasing doping concentration, both bonding and antibonding quasiparticle peaks become sharper and the spectral weights of these peaks increase in intensity. Furthermore, we have also discussed the temperature dependence of the electron spectrum. The result of the electron spectral functions at $[\pi,0]$ point for $t/J=2.5$, $t'/t=0.15$, and $t_\perp/t=0.3$ at $\delta=0.15$ with $T=0.1J$ (solid line), $T=0.05J$ (dashed line), and $T=0.01J$ (dotted line) are plotted in Fig. 3. It is shown obviously that both bonding and antibonding spectral weights are suppressed with increasing temperatures. These results are also qualitatively consistent with the ARPES experimental results on doped bilayer cuprates.[3,9–11]

To consider the quasiparticle dispersion of doped bilayer cuprates, we have made a series of calculations for both bonding and antibonding electron spectral functions at different momenta, and found that the lowest energy peaks are well defined at all momenta. In particular, the positions of both bonding and antibonding quasiparticle peaks as a function of energy ω for momentum $\mathbf{k}$ in the vicinity of the $[\pi,0]$ point are almost not changeable, which leads to the unusual

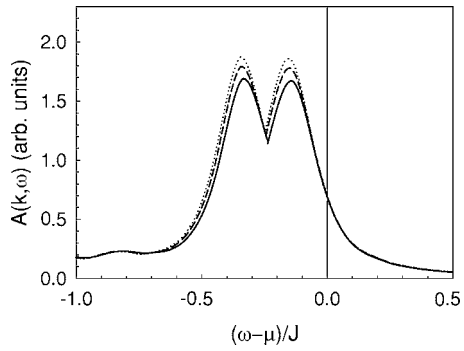

FIG. 2. The electron spectral functions at the $[\pi,0]$ point for $t/J=2.5$, $t'/t=0.15$, and $t_\perp/t=0.3$ with $T=0.1J$ at $\delta=0.09$ (solid line), $\delta=0.12$ (dashed line), and $\delta=0.15$ (dotted line).

quasiparticle dispersion around the $[\pi,0]$ point. To show this broad feature clearly, we plot the positions of the lowest energy quasiparticle peaks in the bonding and antibonding electron spectra as a function of momentum along the high symmetry directions with $T=0.1J$ at $\delta=0.15$ for $t/J=2.5$, $t'/t=0.15$, and $t_\perp/t=0.3$ in Fig. 4. For comparison, the corresponding result from the tight-binding fit to the experimental data of the doped bilayer cuprate $Bi_2Sr_2CaCu_2O_{8+\delta}$ (Ref. 10) is also shown in Fig. 2 (inset). Our result shows that, in analogy to the doped single layer cuprates,[17] both electron bonding and antibonding quasiparticles around the $[\pi,0]$ point disperse very weakly with momentum, and then the two main flatbands appear, while the Fermi energy is only slightly above these flatbands. Moreover, this bilayer energy band splitting reaches its maximum at the $[\pi,0]$ point. This result shows that the bilayer interaction has significant contributions to the electronic structure of doped bilayer cuprates and is in qualitative agreement with those obtained from the ARPES experimental measurements on doped bilayer cuprates.[3,9–11] Within the $t-t'-t''-J$ model, this quasiparticle dispersion of doped bilayer cuprates has been studied based on the resonating valence bond wave function and Gutzwiller approximation,[15] where the quasiparticle dispersion relations are degenerate along the [0, 0]–$[\pi,\pi]$ directions and the splitting becomes maximum at the $[\pi,0]$ point, which is consistent with our present result.

The essential physics of the double-peak structure of the electron spectral function around the $[\pi,0]$ point in the

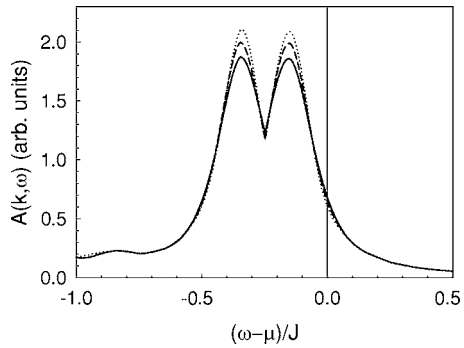

FIG. 3. The electron spectral functions at the $[\pi,0]$ point for $t/J=2.5$, $t'/t=0.15$, and $t_\perp/t=0.3$ at $\delta=0.15$ with $T=0.1J$ (solid line), $T=0.05J$ (dashed line), and $T=0.01J$ (dotted line).

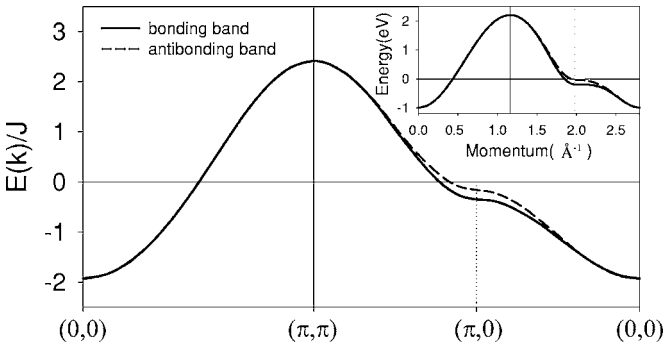

FIG. 4. The positions of the lowest energy quasiparticle peaks in the bonding (solid line) and antibonding (dashed line) electron spectra as a function of momentum with $T=0.1J$ at $\delta=0.15$ for $t/J=2.5$, $t'/t=0.15$, and $t_\perp/t=0.3$. Inset: The corresponding result from the tight-binding fit to the experimental data of the doped bilayer cuprate $Bi_2Sr_2CaCu_2O_{8+\delta}$ taken from Ref. 10.

present doped bilayer cuprates is dominated by the bilayer interaction. The full electron Green's function in doped bilayer cuprates is divided into the longitudinal and transverse parts, respectively, due to the bilayer interaction, thus these longitudinal and transverse Green's functions (hence the bonding and antibonding electron spectral functions and corresponding quasiparticle dispersions) are obtained beyond the MF approximation by considering the dressed holon fluctuation due to the spin-pair bubble. Therefore the nature of the bonding and antibonding electron spectral functions of doped bilayer cuprates in the normal state is closely related to the strong interaction between the dressed holons (hence electron quasiparticles) and collective magnetic excitations. In this case, the single-particle hoppings in the bilayer t-t'-J model are strongly renormalized by the magnetic interaction. As a consequence, both bonding and antibonding quasiparticle bandwidths are reduced to the order of (a few) J, and then the energy scales of both bonding and antibonding quasiparticle energy bands are controlled by the magnetic interaction. These renormalizations for both bonding and antibonding energy bands are then responsible for the unusual bonding and antibonding electron quasiparticle spectra and the production of the two main flatbands around the $[\pi,0]$ point. As in the single layer case, our present results also show that the electron quasiparticle excitations in doped bilayer cuprates originating from the dressed holons and spins are due to the charge-spin recombination; this reflects the composite nature of the electron quasiparticle excitations. Then the unconventional normal-state properties in doped bilayer cuprates are attributed to the presence of the dressed holons, spins, electron quasiparticle excitations, and bilayer coupling.

IV. SUMMARY AND DISCUSSIONS

In conclusion, we have shown that if the strong dressed holon–spin coupling and bilayer interaction are taken into account, the t-t'-J model *per se* can correctly reproduce some main features of the ARPES electron spectrum and the quasiparticle dispersion of doped bilayer cuprates in the normal state. In our opinion, the differentiation between the bonding and antibonding components is essential, which leads to two main flatbands around the $[\pi,0]$ point below the Fermi energy. In analogy to the doped single layer cuprates, the lowest energy states in doped bilayer cuprates are located at the $[\pi/2,\pi/2]$ point. Our results also show that the striking behavior of the electronic structure in doped bilayer cuprates is intriguingly related to the bilayer interaction, together with strong coupling between the electron quasiparticles and collective magnetic excitations.

The experimental[24] and theoretical,[15,18] analyses show that the physical properties for different families of doped cuprates are strongly correlated with t' and $t_\perp$. This means that the different values of parameters t/J, t'/t, and $t_\perp/t$ should be chosen for different families of doped cuprates. For comparison, the values of parameters t/J and t'/t in the present work have been chosen to be the same as in the single layer case.[17] Furthermore, the value of parameter $t_\perp/t$ in the present work is qualitatively consistent with that in the local-density approximation calculations[18] based on the bilayer Hubbard model and the calculations within the bilayer $t-t'$-t''-J model based on the resonating valence bond wave function and Gutzwiller approximation.[15] Although the simplest bilayer t-t'-J model cannot be regarded as a complete model for the quantitative comparison with doped bilayer cuprates, our present results for the normal state are in qualitative agreement with the major experimental observations in the normal state of doped bilayer cuprates.[3,9–11]

Finally, we have noted that the very recent ARPES experiments have shown that although the largest BS is found in the electron spectral function around the $[\pi,0]$ point, a small BS remains also around the $[\pi/2,\pi/2]$ point in a wide doping range.[25,26] It has been argued that the observed small BS around the $[\pi/2,\pi/2]$ point is in good agreement with the local-density-approximation based-band structure calculations, and is caused by the vertical O $2p_\sigma$-O $2p_\sigma$ hopping $t_\perp^{pp}$ between two adjacent planes.[25,26] Therefore the significance of the p-p transfer $t_\perp^{pp}$ should be taken into account. These and related issues are currently under investigation.

ACKNOWLEDGMENTS

The authors would like to thank H. Guo and L. Cheng for helpful discussions. This work was supported by the National Natural Science Foundation of China under Grant Nos. 90403005 and 10547104, and by the funds from the Ministry of Science and Technology of China under Grant Nos. 2006CB601002 and 2006CB921300.

APPENDIX: DRESSED HOLON GREEN'S FUNCTION IN THE BILAYER SYSTEM

As in the single layer case,[17] the full dressed holon Green's function in the doped bilayer cuprates satisfies the equation[21]

$$g(\mathbf{k},\omega)=g^{(0)}(\mathbf{k},\omega)+g^{(0)}(\mathbf{k},\omega)\Sigma^{(h)}(\mathbf{k},\omega)g(\mathbf{k},\omega), \quad \text{(A1)}$$

with the MF dressed holon Green's function $g^{(0)}(\mathbf{k},\omega)=g_L^{(0)}\times(\mathbf{k},\omega)+\sigma_x g_T^{(0)}(\mathbf{k},\omega)$, where the longitudinal and transverse parts are obtained as

$$g_L^{(0)}(\mathbf{k},\omega)=\frac{1}{2}\sum_{\nu=1,2}\frac{1}{\omega-\xi_{\nu\mathbf{k}}}, \tag{A2a}$$

$$g_T^{(0)}(\mathbf{k},\omega)=\frac{1}{2}\sum_{\nu=1,2}(-1)^{\nu+1}\frac{1}{\omega-\xi_{\nu\mathbf{k}}}, \tag{A2b}$$

and the dressed holon self-energy function $\Sigma^{(h)}(\mathbf{k},\omega)=\Sigma_L^{(h)}\times(\mathbf{k},\omega)+\sigma_x\Sigma_T^{(h)}(\mathbf{k},\omega)$, where $\Sigma_L^{(h)}(\mathbf{k},\omega)$ and $\Sigma_T^{(h)}(\mathbf{k},\omega)$ are the corresponding longitudinal and transverse parts, and have been given in Eq. (6). This self-energy function $\Sigma^{(h)}(\mathbf{k},\omega)$ renormalizes the MF dressed holon spectrum, and thus, it describes the quasiparticle coherence. On the other hand, since we only study the low-energy behavior of doped bilayer cuprates, then the quasiparticle coherence can be discussed in the static limit. In this case, we follow the previous discussions for the single layer case[17] and obtain explicitly the longitudinal and transverse parts of the full dressed holon Green's functions of the doped bilayer system as

$$g_L(\mathbf{k},\omega)=\frac{1}{2}\sum_{\nu=1,2}\frac{Z_{FA}^{(\nu)}}{\omega-\bar{\xi}_{\nu\mathbf{k}}}, \tag{A3a}$$

$$g_T(\mathbf{k},\omega)=\frac{1}{2}\sum_{\nu=1,2}(-1)^{\nu+1}\frac{Z_{FA}^{(\nu)}}{\omega-\bar{\xi}_{\nu\mathbf{k}}}, \tag{A3b}$$

with the quasiparticle coherent weights satisfy the following equations:

$$\frac{1}{Z_{FA}^{(1)}}=1+\frac{1}{32N^2}\sum_{\mathbf{q},\mathbf{p}}\sum_{\nu,\nu',\nu''}[1+(-1)^{\nu+\nu'+\nu''+1}]\Lambda_{\nu\nu'\nu''}(\mathbf{q},\mathbf{p}), \tag{A4a}$$

$$\frac{1}{Z_{FA}^{(2)}}=1+\frac{1}{32N^2}\sum_{\mathbf{q},\mathbf{p}}\sum_{\nu,\nu',\nu''}[1-(-1)^{\nu+\nu'+\nu''+1}]\Lambda_{\nu\nu'\nu''}(\mathbf{q},\mathbf{p}), \tag{A4b}$$

where the kernel function $\Lambda_{\nu\nu'\nu''}(\mathbf{q},\mathbf{p})$ can be evaluated as

$$\begin{aligned}\Lambda_{\nu\nu'\nu''}(\mathbf{q},\mathbf{p})=C_{\nu\nu''}(\mathbf{p}+\mathbf{k}_0)Z_{FA}^{(\nu'')}\frac{B_{\nu'\mathbf{p}}B_{\nu\mathbf{q}}}{\omega_{\nu'\mathbf{p}}\omega_{\nu\mathbf{q}}}\\ \times\left(\frac{F_{\nu\nu'\nu''}^{(1)}(\mathbf{q},\mathbf{p})}{[\omega_{\nu'\mathbf{p}}-\omega_{\nu\mathbf{q}}+\bar{\xi}_{\nu''\mathbf{p}-\mathbf{q}+\mathbf{k}_0}]^2}\right.\\ +\frac{F_{\nu\nu'\nu''}^{(2)}(\mathbf{q},\mathbf{p})}{[\omega_{\nu'\mathbf{p}}-\omega_{\nu\mathbf{q}}-\bar{\xi}_{\nu''\mathbf{p}-\mathbf{q}+\mathbf{k}_0}]^2}\\ +\frac{F_{\nu\nu'\nu''}^{(3)}(\mathbf{q},\mathbf{p})}{[\omega_{\nu'\mathbf{p}}+\omega_{\nu\mathbf{q}}+\bar{\xi}_{\nu''\mathbf{p}-\mathbf{q}+\mathbf{k}_0}]^2}\\ \left.+\frac{F_{\nu\nu'\nu''}^{(4)}(\mathbf{q},\mathbf{p})}{[\omega_{\nu'\mathbf{p}}+\omega_{\nu\mathbf{q}}-\bar{\xi}_{\nu''\mathbf{p}-\mathbf{q}+\mathbf{k}_0}]^2}\right),\end{aligned} \tag{A5}$$

with

$$C_{\nu\nu''}(\mathbf{p})=[Z(t\gamma_{\mathbf{p}}-t'\gamma'_{\mathbf{p}})+(-1)^{\nu+\nu''}t_\perp(\mathbf{p})]^2,$$

$$\begin{aligned}F_{\nu\nu'\nu''}^{(1)}(\mathbf{q},\mathbf{p})=n_F(\bar{\xi}_{\nu''\mathbf{p}-\mathbf{q}+\mathbf{k}_0})[n_B(\omega_{\nu'\mathbf{p}})-n_B(\omega_{\nu\mathbf{q}})]\\ +n_B(\omega_{\nu\mathbf{q}})[1+n_B(\omega_{\nu'\mathbf{p}})],\end{aligned}$$

$$\begin{aligned}F_{\nu\nu'\nu''}^{(2)}(\mathbf{q},\mathbf{p})=n_F(\bar{\xi}_{\nu''\mathbf{p}-\mathbf{q}+\mathbf{k}_0})[n_B(\omega_{\nu\mathbf{q}})-n_B(\omega_{\nu'\mathbf{p}})]\\ +n_B(\omega_{\nu'\mathbf{p}})[1+n_B(\omega_{\nu\mathbf{q}})],\end{aligned}$$

$$\begin{aligned}F_{\nu\nu'\nu''}^{(3)}(\mathbf{q},\mathbf{p})=[1-n_F(\bar{\xi}_{\nu''\mathbf{p}-\mathbf{q}+\mathbf{k}_0})][1+n_B(\omega_{\nu\mathbf{q}})\\ +n_B(\omega_{\nu'\mathbf{p}})]+n_B(\omega_{\nu\mathbf{q}})n_B(\omega_{\nu'\mathbf{p}}),\end{aligned}$$

and

$$\begin{aligned}F_{\nu\nu'\nu''}^{(4)}(\mathbf{q},\mathbf{p})=n_F(\bar{\xi}_{\nu''\mathbf{p}-\mathbf{q}+\mathbf{k}_0})[1+n_B(\omega_{\nu\mathbf{q}})+n_B(\omega_{\nu'\mathbf{p}})]\\ +n_B(\omega_{\nu\mathbf{q}})n_B(\omega_{\nu'\mathbf{p}}).\end{aligned}$$

The two equations in Eq. (A4) must be solved together with other self-consistent equations[17] as follows:

$$\delta=\frac{1}{4N}\sum_{\nu,\mathbf{k}}Z_{FA}^{(\nu)}\left(1-\mathrm{th}\left[\frac{1}{2}\beta\bar{\xi}_{\nu\mathbf{k}}\right]\right), \tag{A6a}$$

$$\phi_1=\frac{1}{4N}\sum_{\nu,\mathbf{k}}\gamma_{\mathbf{k}}Z_{FA}^{(\nu)}\left(1-\mathrm{th}\left[\frac{1}{2}\beta\bar{\xi}_{\nu\mathbf{k}}\right]\right), \tag{A6b}$$

$$\phi_2=\frac{1}{4N}\sum_{\nu,\mathbf{k}}\gamma'_{\mathbf{k}}Z_{FA}^{(\nu)}\left(1-\mathrm{th}\left[\frac{1}{2}\beta\bar{\xi}_{\nu\mathbf{k}}\right]\right), \tag{A6c}$$

$$\phi_\perp=\frac{1}{4N}\sum_{\nu,\mathbf{k}}(-1)^{\nu+1}Z_{FA}^{(\nu)}\left(1-\mathrm{th}\left[\frac{1}{2}\beta\bar{\xi}_{\nu\mathbf{k}}\right]\right), \tag{A6d}$$

$$\frac{1}{2}=\frac{1}{4N}\sum_{\nu,\mathbf{k}}\frac{B_{\nu\mathbf{k}}}{\omega_{\nu\mathbf{k}}}\coth\left[\frac{1}{2}\beta\omega_{\nu\mathbf{k}}\right], \tag{A6e}$$

$$\chi_1=\frac{1}{4N}\sum_{\nu,\mathbf{k}}\gamma_{\mathbf{k}}\frac{B_{\nu\mathbf{k}}}{\omega_{\nu\mathbf{k}}}\coth\left[\frac{1}{2}\beta\omega_{\nu\mathbf{k}}\right], \tag{A6f}$$

$$\chi_2=\frac{1}{4N}\sum_{\nu,\mathbf{k}}\gamma'_{\mathbf{k}}\frac{B_{\nu\mathbf{k}}}{\omega_{\nu\mathbf{k}}}\coth\left[\frac{1}{2}\beta\omega_{\nu\mathbf{k}}\right], \tag{A6g}$$

$$C_1=\frac{1}{4N}\sum_{\nu,\mathbf{k}}\gamma_{\mathbf{k}}^2\frac{B_{\nu\mathbf{k}}}{\omega_{\nu\mathbf{k}}}\coth\left[\frac{1}{2}\beta\omega_{\nu\mathbf{k}}\right], \tag{A6h}$$

$$C_2=\frac{1}{4N}\sum_{\nu,\mathbf{k}}\gamma_{\mathbf{k}}\gamma'_{\mathbf{k}}\frac{B_{\nu\mathbf{k}}}{\omega_{\nu\mathbf{k}}}\coth\left[\frac{1}{2}\beta\omega_{\nu\mathbf{k}}\right], \tag{A6i}$$

$$C_3=\frac{1}{4N}\sum_{\nu,\mathbf{k}}\gamma'^2_{\mathbf{k}}\frac{B_{\nu\mathbf{k}}}{\omega_{\nu\mathbf{k}}}\coth\left[\frac{1}{2}\beta\omega_{\nu\mathbf{k}}\right], \tag{A6j}$$

$$\chi_1^z=\frac{1}{4N}\sum_{\nu,\mathbf{k}}\gamma_{\mathbf{k}}\frac{B_{z\nu\mathbf{k}}}{\omega_{z\nu\mathbf{k}}}\coth\left[\frac{1}{2}\beta\omega_{z\nu\mathbf{k}}\right], \tag{A6k}$$

$$\chi_2^z = \frac{1}{4N}\sum_{\nu,\mathbf{k}} \gamma'_{\mathbf{k}} \frac{B_{z\nu\mathbf{k}}}{\omega_{z\nu\mathbf{k}}} \coth\left[\frac{1}{2}\beta\omega_{z\nu\mathbf{k}}\right], \quad \text{(A6l)}$$

$$C_1^z = \frac{1}{4N}\sum_{\nu,\mathbf{k}} \gamma_{\mathbf{k}}^2 \frac{B_{z\nu\mathbf{k}}}{\omega_{z\nu\mathbf{k}}} \coth\left[\frac{1}{2}\beta\omega_{z\nu\mathbf{k}}\right], \quad \text{(A6m)}$$

$$C_2^z = \frac{1}{4N}\sum_{\nu,\mathbf{k}} \gamma_{\mathbf{k}}\gamma'_{\mathbf{k}} \frac{B_{z\nu\mathbf{k}}}{\omega_{z\nu\mathbf{k}}} \coth\left[\frac{1}{2}\beta\omega_{z\nu\mathbf{k}}\right], \quad \text{(A6n)}$$

$$\chi_\perp = \frac{1}{4N}\sum_{\nu,\mathbf{k}} (-1)^{\nu+1} \frac{B_{\nu\mathbf{k}}}{\omega_{\nu\mathbf{k}}} \coth\left[\frac{1}{2}\beta\omega_{\nu\mathbf{k}}\right], \quad \text{(A6o)}$$

$$C_\perp = \frac{1}{4N}\sum_{\nu,\mathbf{k}} (-1)^{\nu+1} \gamma_{\mathbf{k}} \frac{B_{\nu\mathbf{k}}}{\omega_{\nu\mathbf{k}}} \coth\left[\frac{1}{2}\beta\omega_{\nu\mathbf{k}}\right], \quad \text{(A6p)}$$

$$C'_\perp = \frac{1}{4N}\sum_{\nu,\mathbf{k}} (-1)^{\nu+1} \gamma'_{\mathbf{k}} \frac{B_{\nu\mathbf{k}}}{\omega_{\nu\mathbf{k}}} \coth\left[\frac{1}{2}\beta\omega_{\nu\mathbf{k}}\right], \quad \text{(A6q)}$$

$$\chi_\perp^z = \frac{1}{4N}\sum_{\nu,\mathbf{k}} (-1)^{\nu+1} \frac{B_{z\nu\mathbf{k}}}{\omega_{z\nu\mathbf{k}}} \coth\left[\frac{1}{2}\beta\omega_{z\nu\mathbf{k}}\right], \quad \text{(A6r)}$$

$$C_\perp^z = \frac{1}{4N}\sum_{\nu,\mathbf{k}} (-1)^{\nu+1} \gamma_{\mathbf{k}} \frac{B_{z\nu\mathbf{k}}}{\omega_{z\nu\mathbf{k}}} \coth\left[\frac{1}{2}\beta\omega_{z\nu\mathbf{k}}\right], \quad \text{(A6s)}$$

$$C'^z_\perp = \frac{1}{4N}\sum_{\nu,\mathbf{k}} (-1)^{\nu+1} \gamma'_{\mathbf{k}} \frac{B_{z\nu\mathbf{k}}}{\omega_{z\nu\mathbf{k}}} \coth\left[\frac{1}{2}\beta\omega_{z\nu\mathbf{k}}\right]. \quad \text{(A6t)}$$

Then all the order parameters, decoupling parameter α, chemical potential μ, and the quasiparticle coherent weights, are obtained by the self-consistent calculation.

[1] See, e.g., *Proceedings of Los Alamos Symposium*, edited by K. S. Bedell, D. Coffey, D. E. Meltzer, D. Pines, and J. R. Schrieffer (Addison-Wesley, Redwood City, CA, 1990).

[2] See, e.g., M. A. Kastner, R. J. Birgeneau, G. Shirane, and Y. Endoh, Rev. Mod. Phys. **70**, 897 (1998), and references therein.

[3] See, e.g., A. Damascelli, Z. Hussain, and Z.-X. Shen, Rev. Mod. Phys. **75**, 473 (2003), and references therein.

[4] See, e.g., J. Campuzano, M. Norman, and M. Randeira, in *Physics of Superconductors*, edited by K. Bennemann and J. Ketterson (Springer, Berlin, 2004), Vol. II, p. 167, and references therein.

[5] See, e.g., Z. X. Shen and D. S. Dessau, Phys. Rep. **253**, 1 (1995), and references therein.

[6] P. W. Anderson, in *Frontiers and Borderlines in Many Particle Physics*, edited by R. A. Broglia and J. R. Schrieffer (North-Holland, Amsterdam, 1987), p. 1; Science **235**, 1196 (1987).

[7] Z. X. Shen, W. E. Spicer, D. M. King, D. S. Dessau, and B. O. Wells, Science **267**, 343 (1995); D. M. King, Z. X. Shen, D. S. Dessau, D. S. Marshall, C. H. Park, W. E. Spicer, J. L. Peng, Z. Y. Li, and R. L. Greene, Phys. Rev. Lett. **73**, 3298 (1994).

[8] D. S. Dessau, Z. X. Shen, D. M. King, D. S. Marshall, L. W. Lombardo, P. H. Dickinson, A. G. Loeser, J. DiCarlo, C. H. Park, A. Kapitulnik, and W. E. Spicer, Phys. Rev. Lett. **71**, 2781 (1993); D. S. Marshall, D. S. Dessau, A. G. Loeser, C. H. Park, A. Y. Matsuura, J. N. Eckstein, I. Bozovic, P. Fournier, A. Kapitulnik, W. E. Spicer, and Z. X. Shen, *ibid.* **76**, 4841 (1996).

[9] D. L. Feng, N. P. Armitage, D. H. Lu, A. Damascelli, J. P. Hu, P. Bogdanov, A. Lanzara, F. Ronning, K. M. Shen, H. Eisaki, C. Kim, J.-I. Shimoyama, K. Kishio, and Z. X. Shen, Phys. Rev. Lett. **86**, 5550 (2001).

[10] A. A. Kordyuk, S. V. Borisenko, M. Knupfer, and J. Fink, Phys. Rev. B **67**, 064504 (2003); A. A. Kordyuk and S. V. Borisenko, Low Temp. Phys. **32**, 298 (2006).

[11] Y.-D. Chuang, A. D. Gromko, A. Fedorov, Y. Aiura, K. Oka, Yoichi Ando, H. Eisaki, S. I. Uchida, and D. S. Dessau, Phys. Rev. Lett. **87**, 117002 (2001); P. V. Bogdanov, A. Lanzara, X. J. Zhou, S. A. Kellar, D. L. Feng, E. D. Lu, H. Eisaki, J.-I. Shimoyama, K. Kishio, Z. Hussain, and Z. X. Shen, Phys. Rev. B **64**, 180505(R) (2001).

[12] J. C. Campuzano, H. Ding, M. R. Norman, H. M. Fretwell, M. Randeria, A. Kaminski, J. Mesot, T. Takeuchi, T. Sato, T. Yokoya, T. Takahashi, T. Mochiku, K. Kadowaki, P. Guptasarma, D. G. Hinks, Z. Konstantinovic, Z. Z. Li, and H. Raffy, Phys. Rev. Lett. **83**, 3709 (1999).

[13] A. A. Kordyuk, S. V. Borisenko, T. K. Kim, K. A. Nenkov, M. Knupfer, J. Fink, M. S. Golden, H. Berger, and R. Follath, Phys. Rev. Lett. **89**, 077003 (2002).

[14] S. V. Borisenko, A. A. Kordyuk, T. K. Kim, A. Koitzsch, M. Knupfer, M. S. Golden, J. Fink, M. Eschrig, H. Berger, and R. Follath, Phys. Rev. Lett. **90**, 207001 (2003); S. V. Borisenko, A. A. Kordyuk, T. K. Kim, S. Legner, K. A. Nenkov, M. Knupfer, M. S. Golden, J. Fink, H. Berger, and R. Follath, Phys. Rev. B **66**, 140509(R) (2002).

[15] M. Mori, T. Tohyama, and S. Maekawa, Phys. Rev. B **66**, 064502 (2002).

[16] Shiping Feng, Jihong Qin, and Tianxing Ma, J. Phys.: Condens. Matter **16**, 343 (2004); Shiping Feng, Tianxing Ma, and Jihong Qin, Mod. Phys. Lett. B **17**, 361 (2003).

[17] Huaiming Guo and Shiping Feng, Phys. Lett. A **355**, 473 (2006).

[18] O. K. Anderson, A. I. Liechtenstein, O. Jepsen, and F. Paulsen, J. Phys. Chem. Solids **56**, 1573 (1995); A. I. Liechtenstein, O. Gunnarsson, O. K. Anderson, and R. M. Martin, Phys. Rev. B **54**, 12505 (1996); S. Chakarvarty, A. Sudbo, P. W. Anderson, and S. Strong, Science **261**, 337 (1993).

[19] R. B. Laughlin, Phys. Rev. Lett. **79**, 1726 (1997); J. Low Temp. Phys. **99**, 443 (1995).

[20] P. W. Anderson, Phys. Rev. Lett. **67**, 2092 (1991); Science **288**, 480 (2000).

[21] G. M. Eliashberg, Sov. Phys. JETP **11**, 696 (1960); D. J. Scalapino, J. R. Schrieffer, and J. W. Wilkins, Phys. Rev. **148**, 263 (1966).

[22] Feng Yuan, Jihong Qin, Shiping Feng, and Wei Yeu Chen, Phys. Rev. B **67**, 134504 (2003).

[23] J. Kondo and K. Yamaji, Prog. Theor. Phys. **47**, 807 (1972); Shiping Feng and Yun Song, Phys. Rev. B **55**, 642 (1997).

[24] K. Tanaka, T. Yoshida, A. Fujimori, D. H. Lu, Z.-X. Shen, X.-J. Zhou, H. Eisaki, Z. Hussain, S. Uchida, Y. Aiura, K. Ono, T.

Sugaya, T. Mizuno, and I. Terasaki, Phys. Rev. B **70**, 092503 (2004).

[25] A. A. Kordyuk, S. V. Borisenko, A. N. Yaresko, S.-L. Drechsler, H. Rosner, T. K. Kim, A. Koitzsch, K. A. Nenkov, M. Knupfer, J. Fink, R. Follath, H. Berger, B. Keimer, S. Ono, and Y. Ando, Phys. Rev. B **70**, 214525 (2004); A. A. Kordyuk, S. V. Borisenko, A. Koitzsch, J. Fink, M. Knupfer, B. Buechner, and H. Berger, J. Phys. Chem. Solids **67**, 201 (2006).

[26] T. Yamasaki, K. Yamazaki, A. Ino, M. Arita, H. Namatame, M. Taniguchi, A. Fujimori, Z.-X. Shen, M. Ishikado, and S. Uchida, arXiv:cond-mat/0603006 (unpublished).